Iranian Journal of Fuzzy Systems

Volume 17, Number 1, (2020), pp. 77-90

University of Sistan and Baluchestan

Type-2 fuzzy logic based pitch angle controller for fixed speed wind energy system

K. A. Naik[1] and C. P. Gupta[2]

[1] *Faculty in EEE, Vignana Bharathi Institute of Technology, Hyderabad Telangana, India*
[2] *Faculty in EED, Indian Institute of Technology Roorkee, Roorkee, Uttarakhand, India*

anilnaik205@gmail.com, cpg_umist@yahoo.co.in

Abstract

In this paper, an interval Type-2 fuzzy logic based pitch angle controller is proposed for fixed speed wind energy system (WES) to maintain the aerodynamic power at its rated value. The pitch angle reference is generated by the proposed controller which can compensate the non-linear characteristics of the pitch angle to the wind speed. The presence of third dimension in the Type-2 fuzzy logic controller (FLC) membership function offers an additional degree-of-freedom in the design of the Type-2 FLC controller to improve the system performance. The applicability of the proposed controller is evaluated by considering a nonlinear simulation model of the WES which is developed and implemented using OPAL-RT real time digital simulator. The results show that the proposed controller offers better performance than the conventional PI and fuzzy logic controllers.

Keywords: Fuzzy logic controller, output power, pitch angle controller, Type-2 FLC, uncertainty, wind energy system.

1 Introduction

In the recent years, wind power is evolving its significance due to its resourceful and inherent characteristic of reproducible and pollution-free energy against the ever-increasing environmental threats of conventional energy. Moreover, due to the extensive development in wind energy technology, it is becoming more competitive with conventional energy in terms of cost effectiveness. All these factors have motivated the engineers to adopt the renewable energy resources [29] and today, more than 250,000 wind turbines are operating all over the world.

Different types of induction generator based wind power system have been studied [2]. The modern wind power systems are nowadays utilizing mostly the variable-speed (doubly-fed) induction generators but still, the fixed-speed Squirrel-Cage Induction Generators (SCIG) are also being used. Respectively, in Australia, Germany and Denmark about 87MW, 48MW and 47.1MW of installed wind turbines (rated 1.5MW) are SCIG based wind turbines [28].

According to the wind speed, the fixed speed system typically has two operating regions. In partial load region where the wind speed is lower than the rated wind speed, the maximum energy is extracted from the wind turbine (WT) [23]. In the full load region where the wind speed surpasses its rated speed, the generator output power needs to be regulated at the rated value by employing pitch angle controller since generator has limited capacity [13].

Recently, several pitch angle control methods have been suggested to limit the aerodynamic power of the fixed speed wind energy system during the above rated wind speed. The conventional proportional-integral (PI) and proportional-integral-derivative (PID) controller have been often used for the power regulation [3],[7]. The limitation of these controllers is that a highly nonlinear system needs to be linearized around a nominal operating point. But, for disturbances such as sudden change in wind speed the linearized system model does not predict properly, the actual system behaviour. Another method using H-∞ controller has proposed [20], which offer good performance in generating output power of WT. However, it is rather complex compared with other controllers and the parameters need to be redesigned due to changes in weighting functions.

Corresponding Author: K. A. Naik
Received: August 2018 ; Revised: November 2018; Accepted: April 2019.

The sliding mode pitch angle controller has applied to maintain the WT output power at rated level [14]. Although, this controller exhibits robust performance with nonlinear system. But, chattering phenomena caused by the discontinuous part of the control can have a harmful effect on the pitch actuation system. Thus, the fuzzy logic controller (Type-1 FLC) based pitch angle controller has employed for aerodynamic power limitation [21],[18]. Generally, fuzzy rules and membership functions (MFs) are defined based on experts' knowledge and experience. However, once the membership functions have been defined for designing the controller, the uncertainties in actual degree of MFs cannot be modelled [4]. Therefore, there is a need to look for the new methodology to model the uncertainties in the MFs.

Acknowledging the limitations of Type-1 FLC based pitch-angle controller, this paper proposes an interval Type-2 FLC based pitch-angle controller to deal with the issues of uncertainty in MFs and fuzzy rules. The MF of Type-2 fuzzy logic sets (FLSs) are defined with a three-dimensional fuzzy that includes a footprint-of-uncertainty (FOU) [12],[19]. In the controller design, the third dimension of MFs and FOU offer an additional degree-of-freedom and hence, it is possible to handle and model the uncertainties in the MFs and fuzzy rules. In this paper, an attempt has been made by systematically varying the FOU to improve the aerodynamic power at its rated value subjected to wind speed variations. The contribution of the work lies in designing the Type-2 FLC based pitch angle controller and validation using real time digital simulator of OPAL-RT laboratory.

2 Modelling of grid-connected SCIG wind energy system

2.1 Configuration of the system

The single-line diagram of a typical wind energy system consisting of a wind turbine driven SCIG is as shown in Figure 1. The stator winding of the SCIG is connected to the point of common coupling (PCC) through a step-up transformer (0.69/25kV) which exports power to the 120kV grid through step-up transformer (25/120kV) and a transmission line ($R_{TL} + jX_{TL}$) operating at 120kV. The rotor of the SCIG is driven by a variable pitch wind turbine. Hence, pitch-angle controller is employed to maintain the generator output power at its nominal value, when the wind speed exceeds its nominal speed. The reactive power absorbed by SCIG is compensated using capacitor bank (C) connected at the low voltage bus of the wind energy system as shown in Figure 1. The design parameters of the generator and wind turbine are presented in Appendix A.

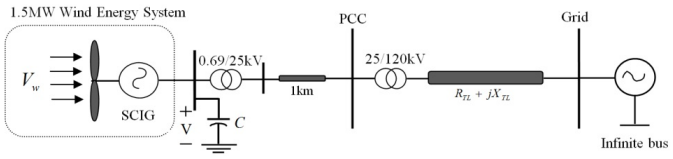

Figure 1: Single-line diagram of the studied grid-connected WES.

2.2 Modelling of wind turbine

The mechanical power developed by the rotor of the wind turbine is directly proportional to the cube of wind speed as

$$P_m = \frac{1}{2}\rho A_r C_p(\lambda, \beta) V_w^3 = C_p P_e \tag{1}$$

The typical wind turbine is characterized by the power coefficient (C_p) which depends upon the ratio of rotor-tip speed (λ)and blade pitch-angle (β). In many literatures, the power coefficient curve has been described by different appropriate equations. In this paper, (C_p) for the studied wind turbine is taken as follows [1]:

$$C_p(\lambda, \beta) = c_1(c_2/\lambda_i - c_3\beta - c_4)\, e^{-c_5/\lambda_i} + c_6\lambda \tag{2}$$

where

$$\frac{1}{\lambda_i} = \frac{1}{\lambda + 0.008\beta} - \frac{0.035}{\beta^3 + 1} \tag{3}$$

The coefficients $c_1 - c_6$ are:$c_1 = 0.5176, c_2 = 116, c_3 = 116, c_4 = 0.4, c_5 = 21 and c_6 = 0.0068$ and the blade tip-speed (λ) is defined as:

$$\lambda = \frac{tip\ speed\ of\ the\ blade}{wind\ speed} = \frac{\omega R}{V_w} \tag{4}$$

where R is the radius of turbine rotor [m], is angular speed of the turbine shaft [rad/s] and is the wind velocity [m/s]. According to in (1) - (4), the power coefficient versus tip-speed ratio ($C_p - \lambda$) curve for different values of the pitch-angle beta (β) of the studied wind turbine is obtained as shown in Figure 2. For different values of wind speed (V_w), the turbine output power versus turbine speed characteristics is as shown in Figure 3. It can be observed from Figure 2 and 3 (which describe the wind turbine characteristics) that the maximum power can be extracted at any wind speed with the help of corresponding optimal rotor speed. Moreover, if the wind speed (V_w) exceeds the rated wind speed, the turbine output power will surpass the rated power and therefore, it is required to reduce the mechanical power of the wind turbine using pitch-control of the wind turbine.

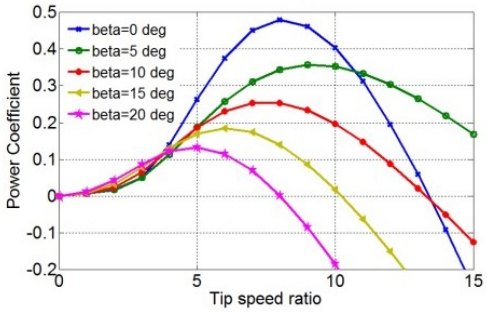

Figure 2: Wind turbine $C_p - \lambda$ curve.

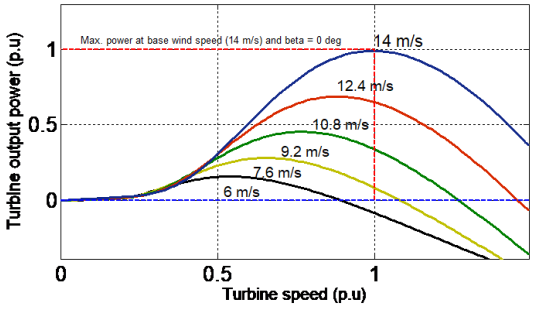

Figure 3: Turbine Power characteristics.

2.3 Wind turbine operating regions

The operating regions of a typical wind turbine system can be divided into four sections as shown in Figure 4. The wind speeds over these regions can be divided into cut-in wind speed (V_{wCI}), rated wind speed (V_{wR}) and cut-out wind speed (V_{wCO}). The values of (V_{wCI}), (V_{wR}) and (V_{wCO}) for the studied wind turbine are 4 m/s, 14 m/s and 25 m/s, respectively. The wind turbine is in sleep state in region I, where the wind speed is lesser than . Region II is called a partial load region where the wind speed (V_w) is higher than (V_{wCI}) but lower than(V_{wR}) .In this region, the main control objective is to extract maximize wind power. The maximum power can be extracted if the power coefficient (C_p) is kept at maximum power coefficient ($C_p max$) obtained with the optimal values of the tip-speed ratio λ and the pitch-angle β i.e.

$$C_{pmax} = C_p|_{\lambda=\lambda_{opt}}^{\beta=\beta_{opt}} \tag{5}$$

For the wind turbine model studied in this paper, the values of ($C_p max$) , (λ_{opt}) and (β_{opt} respectively are computed as 0.48, 8.1 and 0.

In region III, WT extract rated power and called as full load region where pitch angle controller generate a pitch angle to limit the WT output power at rated subjected to wind speed changes. Wind speed greater than (V_{wCO}) named as region IV where WT is stalled (off state).

2.4 Modelling of squirrel-cage induction generator

For the modelling of the SCIG, the a-b-c reference frame is transformed into the d-q axis reference frame. The flux-linkage equations of the studied SCIG driven by the wind turbine can be written in per-unit d-q axis reference frame as follows [1]:

$$p\phi_{ds} = \omega_b \left(V_{ds} + R_s i_{ds} + \phi_{qs} \right) \tag{6}$$

$$p\phi_{qs} = \omega_b \left(V_{qs} + R_s i_{ds} - \phi_{ds} \right) \tag{7}$$

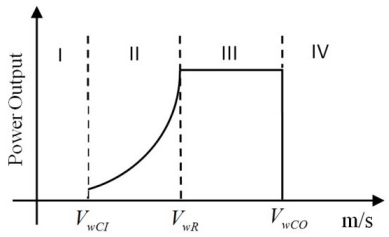

Figure 4: Different operating regions of a studied wind turbine.

$$p\phi_{dr} = \omega_b \left(V_{dr} + R_r i_{dr} \right) + \left(\omega_b - \omega_r \right) \phi_{qr} \tag{8}$$

$$p\phi_{qr} = \omega_b \left(V_{qr} + R_r i_{qr} \right) + \left(\omega_b - \omega_r \right) \phi_{dr} \tag{9}$$

Where, p is the derivative operator. In the above Eqs. (6) - (9), all the variables of the rotor have been referred to the stator side. Then, the per-unit equation of the electromagnetic torque is expressed as:

$$T_e = \phi_{ds} i_{qs} - \phi_{qs} i_{ds} \tag{10}$$

Since generator rotor and wind turbine can be represented as an equivalent mass. Hence, the dynamic equation of motion can be written as.

$$p\omega_m = \frac{\omega_b}{2H} \left(T_m - T_e \right) \tag{11}$$

Where, H is the equivalent inertia constant of both induction generator rotor and wind turbine.

3 Pitch angle controller design

The block diagram of a typical pitch-angle control system for the wind turbine is shown in Figure 5. In general, pitch angle controller regulate the output power of wind turbine when the wind speed (V_{wR}) . The difference between the measured power/electric output power (P_g) and power reference/nominal power (P_g^{REF}) goes through the controller $C(s)$, which regulates the output power in accordance with error ϵ.

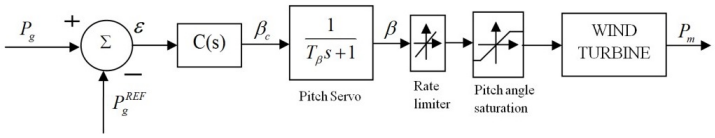

Figure 5: The typical pitch-angle control system.

The pitch-angle control strategy mathematically expressed as follows

$$\beta_c = \frac{\Delta\beta}{\Delta P} \left(P_g - P_g^{REF} \right) + \beta_i \tag{12}$$

Where $\beta_i$is the initial pitch-angle controller, $\Delta\beta$ and ΔP are small-signal state variables of pitch angle and active power, respectively.

The optimum pitch angle β_c from the controller $C(s)$ is used as reference for the pitch actuator/servo system. The purpose of the pitch servo is for proper positioning of the blades. By taking blades direction into account the first order transfer function of the electric or hydraulic pitch servo is as follows:

$$\beta = \frac{1}{(T_\beta s + 1)\beta_c} \tag{13}$$

The blade angle β follows the references pitch β_c or optimum pitch by a first order lag with time constant T_β, which is depends on the pitch actuator. In order to get the realistic response from the pitch control system, the pitch rate and the regulations range of pitch angle are set to $\pm 2^\circ/sec$ and $0^\circ - 45^\circ$, respectively.

It is seen from the Figure 2 that the maximum output power extraction is possible at $\beta = 0^\circ$which is achieved in below rated wind speed. For the above rated wind speed the pitch-angle $\beta$is employed to control the aerodynamic power. Thus, the developed and implemented control strategy for employed controller is presented Eqs. (14) and (15).

$$\beta_c = \frac{\Delta\beta}{\Delta P}\left(P_g - P_g^{REF}\right) + \beta_i \qquad for\ P_g > P_g^{REF} \tag{14}$$

$$\beta_c = \beta_i = 0 \qquad for\ 0 < P_g \leqslant P_g^{REF} \tag{15}$$

In the following sections, the pitch-control design as discussed above is achieved with the help of PI controller, Type-1 FLC and Type-2 FLC so as to compare their performances.

3.1 PI controller design

A PI controller has been designed using linearized model of the wind energy system. The PI controller is used to control the pitch-angle to maintain the output power to the set power (reference power). If the wind speed is under its rated value, there is no generation of pitch angle and hence WES extracts the maximum possible output power. But, in the case wind speed exceeds the rated value, the PI controller increases pitch-angle linearly with respect to wind speed to limit the measured powerP_g to its nominal value. In the present study, Ziegler-Nichols method [26] is used to determine the control gain parameters in an appropriate way.

3.2 Fuzzy logic (Type-1 and Type-2) pitch angle controller design

In this section a typical pitch angle controller is presented in which the wind turbine output power regulated at its rated value during the above rated wind speed. The employed pitch angle controller for both Type-1 and Type-2 FLC is as shown in Figure 6.

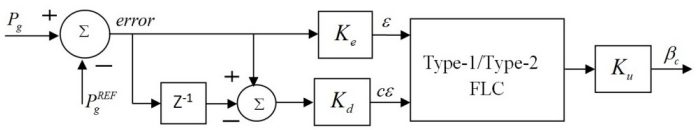

Figure 6: Proposed FLC based pitch angle controller.

The difference between P_g and P_g^{REF} is processed through the fuzzy logic controllers to generate command signal β_c. For convenience, suitable values of the scaling gains ($K_e, K_d\, and K_u$) (of the controller input and output were chosen.

3.3 Design of fuzzy logic controller (Type-1FLC)

In 1965, Professor Lotfi Zadeh has proposed the concept of fuzzy logic (FL) [24]. It has been found to be an excellent choice for many control applications, as it mimics the human control logic. The fuzzy rules are framed on the basis of the expert knowledge gained upon the performance of the system over a time. The block diagram of a conventional FLC (named as Type-1 FLC) is as shown in Figure 7. The fuzzifier converts the crisp value of the input parameter into fuzzy set and depending upon the fuzzy rules framed based on the membership functions for a given parameter of the system and then, fuzzy outputs are obtained with the help of the inference engine. At the end, defuzzifier converts these fuzzy inputs to a crisp output of the FLC to be used for the control purpose.

3.4 Design of interval Type-2 FLC

Quite often, the expert knowledge that is used to construct the rules in a Type-1 FLC is uncertain as the knowledge gained by different experts may or may not be the same. There are three ways in which uncertainty involved with the fuzzy rules can occur are - 1) the rules utilize the words in antecedent and consequent which can mean different things to different people [9], 2) the consequents obtained from the group of experts can be different for the same rule and 3)

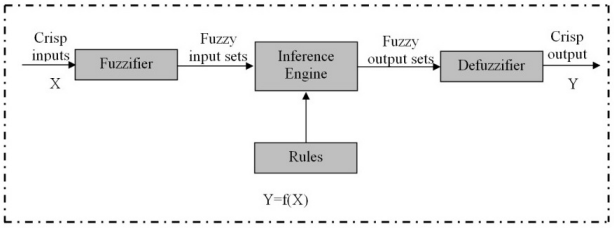

Figure 7: Schematic diagram of classical (Type-1) Fuzzy Logic Controller.

due to noisy training data, uncertainty in antecedent and consequent can transfer into MFs. Therefore, Type-1 FLC, whose membership functions are Type-1 fuzzy sets are unable to handle the uncertainties in the rules. As a result, it may degrade the performance of the Type-1 FLC, especially, when the plant is subjected to the disturbances.

So as to accommodate the uncertainty involved in the expert knowledge, Type-2 FLC is a new technique which offers special features and conquers the limitations of Type-1 fuzzy sets while handling the uncertainties. The primary membership grade of a Type-2 FLC is a Type-1 fuzzy set in [0, 1] and the secondary membership is a crisp number in [0, 1] [17]. The secondary membership function and the range of uncertainty are decided by the third dimension of Type-2 fuzzy sets and footprint-of-uncertainty (FOU), respectively. Thus, in the design of Type-2 FLC, these features can offer additional degree-of-freedom to handle various uncertainties. Hence, wind energy systems, being highly uncertain, can utilize the special features of Type-2 FLCs to improve its operational efficiency during the grid interaction.

3.5 Elementary concept of interval Type-2 fuzzy sets

As explained in [8], if all the distribution points which sit on the FOU is uniform, then the resulting type-2 fuzzy sets are called interval type-2 fuzzy sets [11]. These fuzzy sets have less computational complexity with secondary memberships, made either zero or one. Such sets are the most widely used type-2 fuzzy sets to date [10].

An interval type-2 fuzzy set (denoted) can be characterized with a Type-2 MF $\mu_{\tilde{A}}(x,u)$ can be described as

$$\tilde{A} = \{((x,u), \mu_{\tilde{A}}(x,u)) \; \forall x \in X, \forall u \in J_x \subseteq [0,1]\} \tag{16}$$

Where $x \in X, u \in J_x \subseteq [0,1] and 0 \leq \mu_{\tilde{A}}(x,u) \leq 1$. $\tilde{A}$ can also be characterized as

$$\tilde{A} = \int_{x \in X} \int_{u \in J_x \subseteq [0,1]} \frac{\mu_{\tilde{A}(x,u)}}{(x,u)} \tag{17}$$

Where $x \in X$ and $u \in U$ are the primary and secondary variables, respectively. The secondary variable has domain J_x at each $x \in X$; J_x is called the primary membership.

Equation (17) means $\tilde{A} : X \rightarrow ([a,b] : 0 \leq a \leq b \leq 1)$. The union of all primary memberships is called the footprint-of-uncertainty (FOU) of $\tilde{A}$ and is shown as the shaded region of Figure 8.

$$FOU(\tilde{A}) = \cup_{\forall x \in X} J_x = \{(x,u) : u \in J_x \subseteq [0,1]\} \tag{18}$$

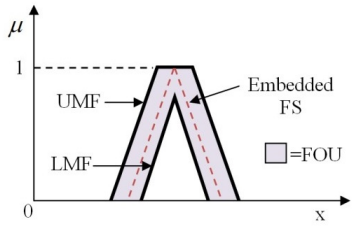

Figure 8: Type-2 Fuzzy Sets with FOU and Embedded Fuzzy Set (FS).

The FOU of Type-2 fuzzy set ($\tilde{A}$) has bounded by two Type-1MFs called as lower membership function (LMF) and the upper membership function (UMF). The UMF and LMF are denoted as $\bar{\mu}_{\tilde{A}}(x)$ and $\underline{\mu}_{\tilde{A}}(x)$ respectively, and are

defined as follow:

$$\bar{\mu}_{\tilde{A}}(x) = \overline{FOU(\tilde{A})} \quad \forall_{x \in X} \tag{19}$$

$$\underline{\mu}_{\tilde{A}}(x) = \underline{FOU(\tilde{A})} \quad \forall_{x \in X} \tag{20}$$

Note that $\in J_x$ is an interval set; i.e.

$$J_x = \left\{(x,u) : u \in \left[\underline{\mu}_{\tilde{A}}(x), \bar{\mu}_{\tilde{A}}(x)\right]\right\}, \tag{21}$$

An embedded fuzzy set (FS) $\tilde{A_e}$ for a continuous universe of discourse X and u is expressed as

$$\tilde{A_e} = \int_{x \in X} [1/u]/x, \quad u \in J_x \tag{22}$$

The set $\tilde{A_e}$ is embedded in $\tilde{A}$ in such a way that the secondary MF is always one at each value of x . A large number of such embedded Type-1 fuzzy set (FS) are combined to form the Type-2 FS. According to [19] the Type-2 FS can be considered as a combination of many different Type-1 FSs where each Type-1 FS is embedded to form the FOU.

3.6 Type-2 FLC design for the studied wind energy system

The Figure 9 shows the steps involved in the Type-2 FLC design algorithm.

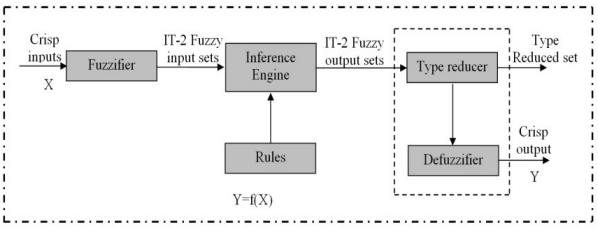

Figure 9: Schematic diagram of Type-2 FLC.

At first, with help the of various membership functions the crisp input is converted to fuzzy inputs using Type-2 membership functions of various system parameters so as to account for the uncertainty involved in the expert knowledge. Then using logical operators, a set of fuzzy rules have been framed to combine the fuzzy output sets into a single set under the inference mechanism. The output of inference engine is converted to Type-1 under type reduction operation and then, the Type reduced sets are converted back to crisp value using various defuzzification techniques as done in the Type-1 FLC. The detailed procedure of designing the Type-2 FLC for the given wind an energy system is as follows:

The MFs and rules are framed for the Type-1 and Type-2 FLCs as given in Figure 10 and Table 1, respectively. The triangular MFs with overlap used for the input and output fuzzy sets. For all the inputs and outputs the universe of discourse is chosen as [-1, +1].

3.7 Fuzzification

As shown in the schematic diagram of the controller configuration (Figure 6), the input and output variables used for the controller design are expressed with the help of fuzzy sets using seven triangular linguistic variables MFs. Notation for the fuzzy sets as: LP (Large Positive), MP (Medium Positive), SP (Small Positive), Z (Zero), SN (Small Negative), MN (Medium Negative), LN (Large Negative). The MFs are selected based on prior knowledge and observations from the various simulation results. The width of the FOU is decided by observing its effect on the WES output power fluctuations. The similar MFs and rules have been designed for Type-1 and Type-2 FLCs to distinguish their performance.

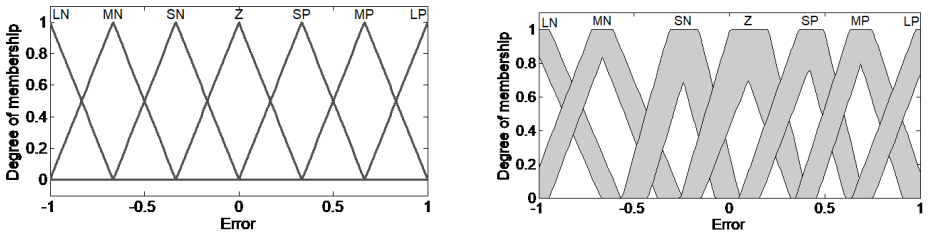

(a) Inputs (ε and cε) and output (β_c). (b) Inputs (ε and cε) and output (β_c).

Figure 10: Designed MFs of inputs and output (a) Type-1 FLC (b) Type-2 FLC.

Table 1: Fuzzy rules table for (β_c).

Error (ε)	Change in Error ($c\varepsilon$)						
	LN	MN	SN	Z	SP	MP	LP
LM	LN	LN	LN	LN	MN	SN	Z
MN	LN	LN	LN	MN	SN	Z	SP
SN	LN	LN	MN	MN	Z	SP	MP
Z	LN	LN	MN	Z	MP	MP	LP
SP	MN	SN	Z	SP	MP	LP	LP
MP	SN	Z	SP	MP	LP	LP	LP
LP	Z	SP	MP	LP	LP	LP	LP

3.8 Fuzzy logic rules/Inference engine

The major function in the inference engine is the rules' implementation, aggregation and Type reduction. With the help of the experts' knowledge on the pitch-angle control of the wind energy system, control strategies is framed as a set of IF-THEN rules and are as:

If (ϵ is x_1) and (ϵ is y_1) then (β_c is w_1)

Similarly, 49 rules have been defined for all input-output MFs as shown in Table 1. In the Type-2 FLCs, the union and intersection functions are defined by join and meet operations to map the input and output sets with fired rules. Therefore, the inference engine utilizes respectively, min-method and max-method for meet and join operations, respectively. Using the extension principle, a detailed mathematical relation between the meet and join operations has presented in [17]. During the aggregation operation, all the fired rules are converted to become a single output fuzzy set. However, the output of inference engine cannot be converted directly to crisp value due to computational limitations. As a result, Type reduction (TR) method has been suggested in the Type-2 FLC system to convert from Type-2 output fuzzy sets to Type-1 fuzzy sets first, and thereafter the normal defuzzification techniques can be applied. Height, center-of-sets, center-of-sums and modified-height are the most accepted TR methods [6], in which centroids of the embedded Type-2 sets are calculated. If larger the FOU width, the number of embedded fuzzy sets increases and this leads to increase in the computational time of TR method. In our present work 'height' TR method has been used for the calculation of the centroid of Type-2 FLCs as it involves much lesser computations as compared to other methods [6].

3.9 Defuzzification

The common defuzzification methods used for the Type-2 FLC are the first (or last) of maxima, centroid-of-area and mean-of-max methods. In this study, centroid-of-area method has been utilized which is the most reasonable and popular method among the others. The centroid of the Type-2 fuzzy set is the collection of centroids of all of its

embedded sets. The defuzzification method converts the output fuzzy to crisp value. The final output of the controller is defined as

where $\beta'_c = \frac{\Delta\beta}{\Delta P}\left(P_g - P_g^{REF}\right) + \beta_i$

The starred value is the final output of the pitch controller, whereas the prime term is the outputs of the Type-2 fuzzy controller.

$$\beta^* = \frac{1}{T_\beta s + 1}\beta'_c \tag{23}$$

4 Real time simulation

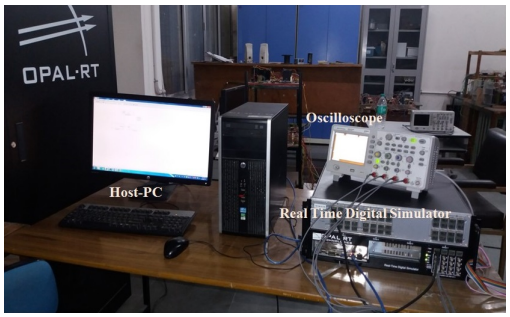

Figure 11: Hardware implementation of studied system.

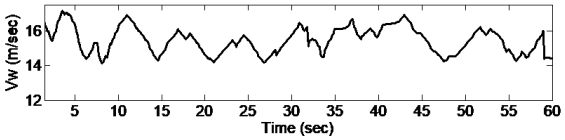

Figure 12: Wind profile.

The real time simulation of the studied system is carried using OPAL-RT digital simulator which is based on RT-lab platform as shown in Figure 11. It consists of OP5600 hardware simulator with one processor and four 3.33-GHz dedicated cores to perform parallel computations. The RT-lab is fully integrated with MATLAB/Simulink, provides the flexibility and scalability to achieve the most complex real-time simulation applications in the power systems, power electronics, automotive, aerospace and industries [22],[15],[27]. The simulator uses advanced fixed time step solvers (ARTEMIS) for strict constraints of real-time simulation of stiff systems. The sampling time used to realize the system is $50\mu s$ To run the models in real time simulation, the RT-lab allows user to readily convert simulink models through real time workshop (RTW). The steps involved for implementation of MATLAB/Simulink model to real time have been provided detail in [16]. The implemented hardware system shown in Figure 11 consists of host personal computer (Host-PC), target (real time digital simulator) and oscilloscope. In the host computer the studied system as shown in Figure 1 has been designed [25]. After that the model has compiled with RT-lab and user interface is done. In real time digital simulator, model execution process has done and results are display in oscilloscope/opcomm (console subsystem).

For the below rated wind speed, the pitch angle controller is not in operation and WT extract maximum power from the wind. But, in general the pitch angle controllers are employed to limit the WT output power at rated level when the wind speed exceeds its nominal value. Therefore, in this work the above rated wind speed pattern is employed as shown in Figure 12. Under this wind speed characteristics, the performance of the PI, Type-1 FLC and the proposed Type-2 FLC were investigated and the real time simulation results were obtained through opcomm block as shown in Figures $13(a)(e)$.

On comparing Figure 13(a), it is observed that the active power output of the wind energy system is having almost identical variations with all three types of controller but real power fluctuations around the rated value with Type-2

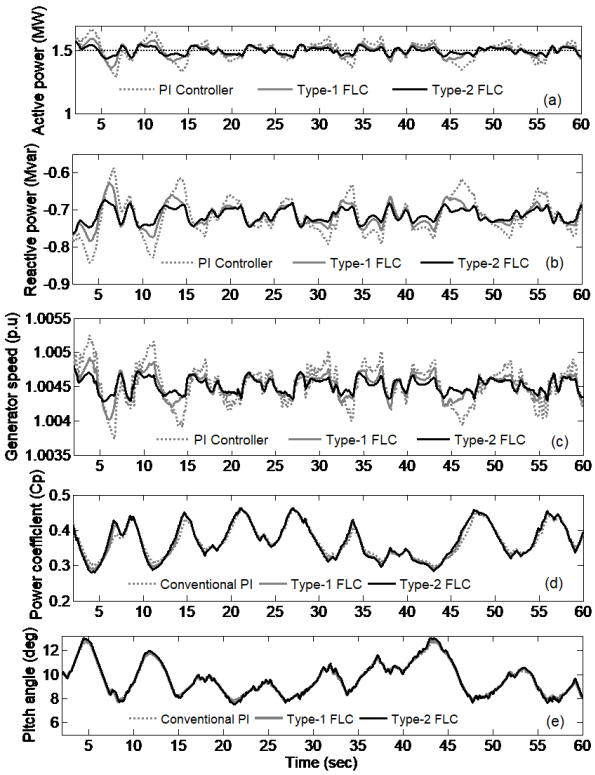

Figure 13: The studied system dynamic responses under the wind speed variations (a) Generator active power (b) Generator reactive power (c) Generator rotor speed (d) Power coefficient (e) Pitch angle.

FLC is considerably smaller than that the PI and Type-1FLC. Consequently, the quality of output power with proposed controller is more favorable since it has lower overshoot characteristics than PI and Type-1. Similarly, Figure 13(b) illustrates the reactive power exchange of the wind energy system with power system network. The fluctuations in the reactive power due to wind speed variations also have been reduced using proposed controller. The Figure 13(c) shows the generator rotor speed where the proposed controller gives good results compared to PI and Type-1 in maintaining the rotor speed at the rated level. The power coefficient of wind turbine with conventional PI, Type-1 and Type-2 controllers are as shown in Figure 13(d). The power coefficient with PI, Type-1 and Type-2 FLC varies according to the pitch angle variations in order to regulate the output power. The pitch angle profiles of the WES with employed controllers are as shown Figure 13(e).

The output power of WES with conventional PI, Type-1 and Type-2 FLCs are also observed in the digital oscilloscope. According to the pitch angle activity of PI, Type-1 and Type-2 FLCs the regulated generator output power has also observed in the oscilloscope as shown in Figures 14(a), (b) and (c).

To investigate the performance of the proposed controller with PI and Type-1 FLC the maximum energy function is calculated. The numerical representation of energy function expressed as follows [18]:

$$P_{max} = \int_0^T P_g(t)dt \tag{24}$$

Where, P_g is the generated output power and T is the total simulation time. In Eq. (24) P_{max} is the integration of the generated output power P_g. If the P_{max} is large, the efficiency of the WT is improved.

Figure 15 shows the energy function results obtained with all the controllers. The maximum energy has been obtained with proposed controller. The energy generation of WES during the 60sec has calculated for all the controllers using Eq. (24). The proposed controller gives approximately 3.12% and 1.31% higher output power than the PI and Type-1, respectively.

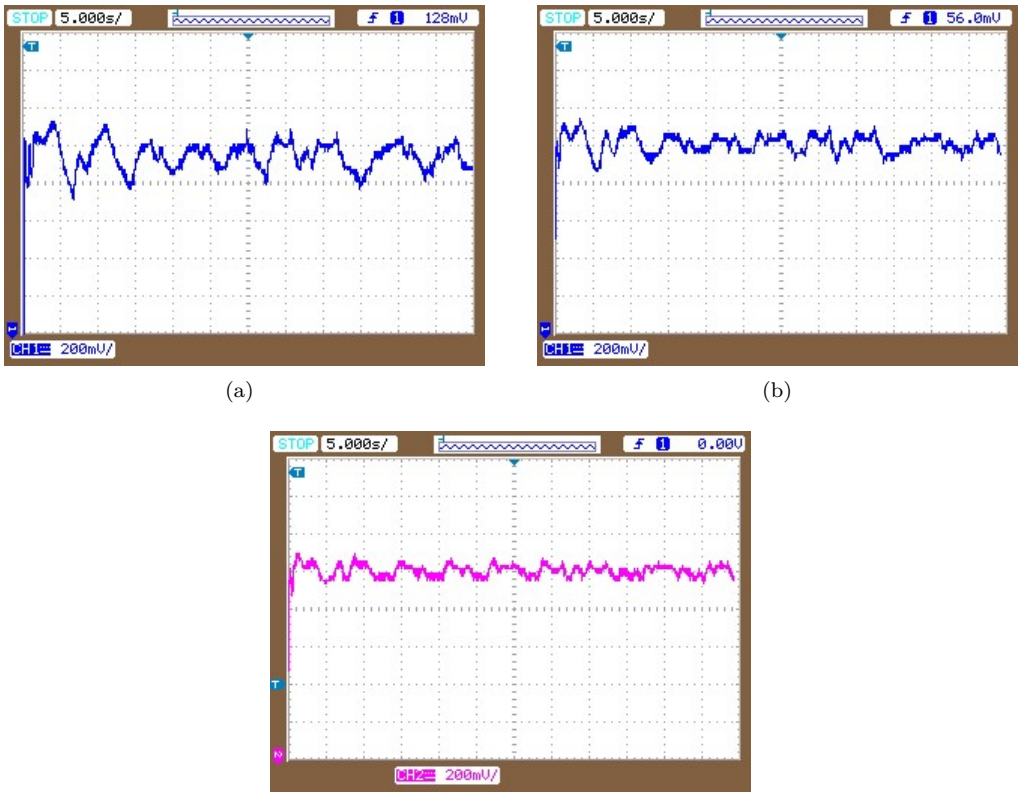

Figure 14: Generator active power obtained in oscilloscope, (a) PI controller (b) Type-1 FLC, (c) Type-2 FLC.

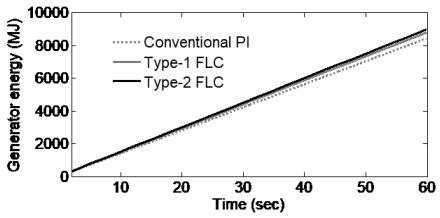

Figure 15: Wind profile.

5 Conclusion

In this paper, an interval Type-2 fuzzy logic technique is developed and proposed for pitch angle controller of fixed speed WES. The proposed controller has a degree of freedom to design the third dimensional membership function and foot print of uncertainties. As the proposed technique has a uniform distribution points sit on the FOU and thus it offers lesser computation with good accuracy. In order to examine the effectiveness of the proposed method in comparison, two well known methods such as PI controller design using Ziegler-Nichols and fuzzy logic methods are implemented. Using OPAL-RT technologies lab, a real time digital simulation environment is developed for the studied system. The real time simulation results were obtained with different control techniques for their real time application. The proposed advanced fuzzy logic controller offered better performance than conventional PI and Type-1 FLC. The applicability of the proposed method with pitch angle control system in case of WES has achieved well power regulation to limit power overloads which can reduce the aerodynamic and mechanical loads on the WT thereby increase the useful life of the turbines themselves. The maximum energy function also has incorporated to investigate the performance of the controllers. The output power of the proposed controller is 3.12% and 1.31% higher than PI and Type-1 FLC, respectively.

6 Acknowledgements

One of the authors, Kanasottu Anil Naik, is a EEE faculty of Vignana Bharathi Institute of Technology (VBIT), Hyderabad, acknowledges DST for providing computational facilities under its FIST program at VBIT Hyderabad, where the computational work has been carried out.

Appendix A

Table 2: Wind turbine parameters [28].

Parameters	Values
Rated power	1.5 MW
Rotor diameter	64 m
Number of blades	3
Cut-in wind speed (V_{wCI})	4 m/s
Cut-out wind speed (V_R)	25 m/s
Rated wind speed (V_{wR})	14 m/s
Generator	SCIG

Table 3: SCIG generator parameters [5].

Parameters	Values
P_{rated}, V_{rated}	1.5 MW, 0.69 kV
R_s, R_r	0.004843 p.u., 0.004377 p.u.
L_s, L_r	0.1248 p.u., 0.1791 p.u.
L_m, H	6.77 p.u., 5.04(s)
C_{wf}	200 kVAR

References

[1] T. Ackerman, *Wind power in power system*, John Wiley & Sons. Ltd, 2005.

[2] F. P. De Mello, J. W. Feltes, L. N. Hannett, J. C. White, *Application of induction generators in power system*, IEEE Transactions on Power Apparatus and Systems, **101**(9) (1982), 3385–3393.

[3] M. Q. Duong, F. Grimaccia, S. Leva , M. Mussetta, E. Ogliari, *Pitch angle control using hybrid controller for all operating regions of SCIG wind turbine system*, Renewable Energy, **70** (2014), 197–203.

[4] H. Hagras, C. Wagner, *Towards the wide spread use of Type-2 fuzzy logic systems in real world applications*, IEEEIEEE Computational Intelligence Magazine, Ixtapa, **7** (2012), 14–24.

[5] M. H. Haque, *Evaluation of power flow solutions with fixed speed wind turbine generating systems*, Energy Conversion and Management, **79** (2014), 511–518.

[6] N. N. Karnik, J. M. Mendel, *Type-2 fuzzy logic systems*, IEEE Transactions on Fuzzy, **7** (1999), 643–658.

[7] K. M. S. Y. Konara, M. L. Kolhe, *Pitch controller modeling for wind turbine power regulation using feed forward control strategies*, IEEE PES Asia-Pacific Power and Energy Engineering Conference (APPEEC), Brisbane, QLD, (2015), 1–5.

[8] J. M. Mendel, *Fuzzy logic systems for engineering: A tutorial*, Proceeding IEEE, **83**(3) (1995), 345–377.

[9] J. M. Mendel, *Computing with words when words can mean different things to different people*, Int. ICSC Congress Computational Intelligence: Methods Applicat, 3rd Annual Symposium, Fuzzy Logic Applicat, (1999), 1–7.

[10] J. M. Mendel, *Computing derivatives in interval Type-2 fuzzy logic systems*, IEEE Transactions on Fuzzy Systems, Ixtapa, **12**(1) (2004), 84–98.

[11] J. M. Mendel, R. I. B. John, *Interval Type-2 fuzzy logic systems made simple*, IEEE Transactions on Fuzzy System, **10**(2) (2006), 117–127.

[12] J. M. Mendel, R. I. John, F. Liu, *Interval Type-2 fuzzy logic systems made simple*, IEEE Transactions on Fuzzy Systems, **14** (2006), 808–821.

[13] Y. Mi, X. Bao, E. Jiang, W. Deng, J. Li, L. Ren, P. Wang, *The pitch angle control of squirrel-cage induction generator wind power generation system using sliding mode control*, 16th European Conference on Power Electronics and Applications, Lappeenranta, (2014), 1–10.

[14] Y. Mi, X. Bao, Y. Yang, H. Zhang, P. Wang, *The sliding mode pitch angle controller design for squirrel-cage induction generator wind power generation system*, Proceedings of the 33rd Chinese Control Conference, Nanjing, (2014), 8113–8117.

[15] S. Mikkili, A. K. Panda, *Types-1 and -2 fuzzy logic controllers-based shunt active filter Id–Iq control strategy with different fuzzy membership functions for power quality improvement using RTDS hardware*, IET Power Electron, **6**(4) (2013), 818–833.

[16] S. Mikkili, A. K. Panda, J. Prattipati, *Review of real-time simulator and the steps involved for implementation of a model from MATLAB/SIMULINK to real-time*, Journal of The Institution of Engineers (India): Series C, (2014), 1–18.

[17] M. Mizumoto, K. Tanaka, *Some properties of fuzzy sets of type 2*, Information and Control, **31**(4) (1976), 312–340.

[18] S. M. Muyeen, J. Tamura, T. Murata, *Stability augmentation of a grid connected wind farm*, Springer-Verlag London Ltd, 2009.

[19] L. Qilian, J. M. Mendel, *Interval Type-2 fuzzy logic systems: Theory design*, IEEE Transactions on Fuzzy Systems, Ixtapa, **8** (2000), 535–550.

[20] R. Sakamoto, T. Senjyo, T. Kaneko, N. Urasaki, T. Takagi, S. Sugimotol, *Output power leveling of wind turbine generator by pitch angle control using H-control*, IEEE Power Systems Conference and Exposition, (2006), 1–6.

[21] D. C. Vega, J. A. Marin, R. T. Sanchez, *Pitch angle controllers design for a horizontal axis wind turbine*, IEEE International Autumn Meeting on Power, Electronics and Computing (ROPEC), Ixtapa, (2015), 1–6.

[22] P. Venne, J. N. Paquin, J. Belanger, *The what, where and why of real-time simulation*, In Proc. IEEE PES General Meeting, (2010), 37–49.

[23] D. Wu, Y. Li, Z. Ji, *Modeling and MPPT control of squirrel-cage induction generator wind power generation system via VisSim*, Chinese Control and Decision Conference, Guilin, (2009), 48–53.

[24] L. A. Zadeh, *Fuzzy sets*, Information and Control, **8** (1965), 338–353.

[25] Y. Zhao, L. Shi, Y. Ni, L. Yao, *Modeling and real-time simulation of wind farm*, Journal of The Institution of Engineers (India): Series C, (2012), 1–4.

[26] J. G. Ziegler, N. B. Nichols, *Optimum settings for automatic controllers*, The American Society of Mechanical Engineers, **65** (1942), 433–444.

[27] RT-LAB Version 10.7.0.361 User Guide, Opal-RT, IIT Roorkee, Uttarakhand, India.

[28] http://www.thewindpower.net/windfarm_en_86_challicum-hills.php, (2017), accessed 21.03.2018.

[29] http://www.gwec.net/global-Fig.s/wind-in-numbers/, The Global Wind Energy Council Belgium, (2017), accessed 25.04.2018.